Manuscript Submitted to:
Composites Science and Technology

Mechanics, Optics, and Thermodynamics of Water Transport in Chemically Modified Transparent Wood Composites

Kyle E. O. Foster [a], *Rollin Jones* [b], *Garret M. Miyake* [c], *Wil V. Srubar III* [a,b,*a] Materials Science and Engineering Program, University of Colorado Boulder, UCB 596, Boulder, CO 80309 USA, [b] Department of Civil, Environmental, and Architectural Engineering, University of Colorado Boulder, ECOT 441 UCB 428, Boulder, CO 80309 USA, [c] Department of Chemistry, Colorado - State University, 301 West Pitkin Street, Fort Collins, CO, 80523 USA

Abstract. Effects of chemical modification on mechanical, optical, and water transport behavior of transparent wood composites (TWCs†) were investigated. TWCs were produced from a methacrylate resin and balsa wood templates using two delignifying pretreatments, namely lignin-oxidation and lignin-modification, and three interfacial modifications, namely acetylation, methacrylation, and treatment with 2-hydroxyethyl methacrylate. Water transport behavior was investigated *via* immersion at three temperatures, where diffusion coefficients, kinetic rate constants, and activation energies of water diffusion were obtained. Lignin-modified TWCs were generally more water resistant than lignin-oxidized TWCs. Interfacial modification of the wood template *via* acetylation and methacrylation were observed to further decrease diffusion coefficients and increase activation energies of diffusion compared to unmodified TWCs, indicating superior fiber-matrix compatibility and improved moisture resistance relative to other tested TWCs. Flexural properties of post-dried TWCs were not adversely affected by moisture compared to samples unconditioned by water. TWC optical properties were measured in pre-immersion, water-saturated, and post-dried states to characterize deterioration of transmittance and haze. While moisture saturation degraded optical properties, optical performance of select TWC classes were observed to rebound upon drying.

* Corresponding Author, T +1 303 492 2621, F +1 303 492 7317, E wsrubar@colorado.edu

† Abbreviation list – TWC: Transparent wood composite, WT: Wood template, LO: Lignin-oxidized, LM: Lignin-modified, U: unmodified, A: acetylated, M: methacrylated, H: 2-hydroxyethyl methacrylate-treated

Keywords: transparent wood, transport properties, hygrothermal effect, surface treatments

1. Introduction

Transparent wood composites (TWCs) are a class of composite materials where delignified bulk wood is impregnated with a polymer that has a refractive index similar to cellulose ($n \approx 1.5$) to produce light-transmitting, continuous-fiber reinforced composites [1–3]. This duality of light transmittance and good mechanical properties has garnered attention for structural material alternatives for glass or transparent plastics. TWCs have potential advantages in applications suited for lower thermal conductivities, diffuse illumination, and lower environmental impacts [4–6].

Implementation of a wood template (WT) as reinforcement in polymer matrices leverages the hierarchical structure of wood, which contributes mechanical integrity, but necessitates modification for TWC applications. The strength of wood primarily comes from aligned cellulose fibrils, contained within a support matrix of hemicellulose and lignin. Given that lignin contributes to coloration *via* visible light absorption in wood, it must be removed or altered to achieve adequate optical transmittance [7]. Several types of delignifying pretreatments are used in the literature [2,3,7]. In addition, others have explored additional chemical modifications to the WT [6,8–10], polymer variation [3,11], nanoparticle additives [12,13], wood species (e.g., balsa wood, basswood, birch, ash, pine), fabrication techniques [14,15], and performance evaluations of TWCs [4,16,17], for multiple applications that require different physical, chemical, and mechanical characteristics.

1.1. Moisture-induced deterioration in wood-polymer composites

Wood-polymer composites in high-humidity and wet environments are susceptible to moisture-induced deterioration. Moisture swells and mechanically softens natural fibers, which can impart permanent damage to the fiber-matrix interface and negatively affect mechanical properties and dimensional stability. Much of the work investigating moisture effects on wood-polymer composites pertains to wood-flour reinforced polypropylene or polyethylene matrices [18–21]. Size, distribution,

and volume fraction of filler affect maximum moisture contents and rate of sorption, where larger particles and higher volume fractions tend to increase maximum theoretical moisture content and sorption rates [19–21]. These findings suggest that the continuous WT of TWCs would lead to greater moisture uptake and more rapid water transport kinetics compared to discrete-fiber composites of equivalent lignocellulosic content [18–20].

Studies have shown that the mechanical properties of wood-polymer composites decrease with moisture exposure [22–24]. Upon moisture intrusion, wood fibers swell and soften, thereby damaging the fiber-matrix interface. The reduction in mechanical properties has often been observed to be non-recoverable, given that saturated-then-dried composites do not regain mechanical properties after initial damage is incurred by moisture intrusion [25]. Moisture sorption in TWCs is expected to not only affect the mechancial, but the optical properties as well as water has a mismatched refractive index ($n = 1.33$) relative to the TWC phases ($n \approx 1.5$). Understanding the influence of moisture sorption on the properties of TWCs will further define suitable applications for these materials and enable development of strategies to mitigate damage.

1.2. Fiber-Matrix Interfacial Modification

Researchers have previously investigated fiber and/or matrix chemical modifications to improve the fiber-matrix interface and, thus, the overall mechanical and moisture resistance properties of wood-polymer composites. Common treatments involve grafting maleate or silane groups to the lignocellulosic fiber component to compatibilize with the polymer matrix, which results in resistance to moisture uptake [18–21,26–28]. Other methods include acetylation and methacrylation of the numerous lignocellulosic hydroxyl groups to increase the hydrophobicity of the filler [29–31].

Many studies on TWCs highlight applications as windows and in photovoltaic assemblies, where durability in moisture-rich environments is required. Given that good light transmittance in TWCs is enabled, in large part, by interfacial compatibility between the WT and the polymer matrix,

understanding potential moisture-induced effects on the optical and mechanical properties of these materials is vital. Robust interfacial interactions between the WT and the resin are desired to minimize photon scattering and maximize load transfer between phases. Moisture intrusion in wood-polymer composites will also affect the dimensional stability of the composite and could lead to substantial swelling or shrinkage with moisture sorption and desorption. Of the numerous studies involving interfacial chemical compatibilization of wood/fibers with a polymer matrix, only a few studies apply these principles in the context of TWCs and, to the best of the authors' knowledge, none have covered compatibilization beyond acetylation of the WT[6,8–10] or specifically investigated long-term (>48 hour) moisture resistance of TWCs [11].

1.3. Scope of Work

In this work, we analyzed the effects of fiber-matrix interfacial chemical modifications on the optics and mechanics, as well as the kinetics and thermodynamics of water transport properties of TWCs. TWCs fabricated using two delignifying pretreatments and three interfacial modifications were subjected to isothermal water immersion until saturation. The two delignifying pretreatments chosen aim to (1) preferentially remove lignin (chlorite oxidation) or (2) bleach the lignin color (hydrogen peroxide oxidation) in order to make the WT suitable for TWC fabrication. The difference in lignin content between the two delignifying pretreatments is anticipated to have an effect on mechanical, optical, and water transport properties in the resulting TWCs. Acetylation of the WT and infiltration with methacrylate polymers has been shown to improve the optical properties of the TWC [6,8,10]. Building on the idea of tailoring the interfacial interactions in TWCs to improve optical properties, two additional modifications are proposed: (a) methacrylation of the WT and infiltration with methacrylate polymers to form covalent linkages between the two phases and (b) addition of 2-hydroxyethyl methacrylate (HEMA) is expected to form hydrogen bonds with wood template while being polymerized into the infiltrated methacrylate polymer. The three

modifications outlined (acetylation, methacrylation, HEMA treatment) were selected to vary the interfacial bonding interactions between the WT in the infiltrating methacrylate polymer and test for their effect on optical properties in the resulting TWCs as well as mechanical properties and water sorption behavior. Water diffusion behavior of TWCs was first categorized and subsequently modeled with mathematical expressions for Fickian diffusion (see supporting information for more details). Activation energies of moisture diffusion were calculated using Arrhenius relationships, enabling quantitative comparison of the effectiveness of modifying the WT. Finally, the effects of moisture and chemical modification on preservation of transmittance, haze, and flexural properties of unmodified and modified TWCs were investigated and reported herein.

2. Materials and methods

2.1. Materials

Balsa wood (Midwest Products) with a thickness of ~1.6 mm and a density of 0.184 g/cm^3 were obtained from a local hardware store (Boulder, CO USA). Clear, photocurable methacrylate-based resin was obtained from Formlabs (RS-F2-GPCL-04). Sodium chlorite, sodium acetate, sodium silicate, ethylenediaminetetraacetic acid (EDTA), acetyl chloride (AcCl), methacryloyl chloride (MeCl), 2-hydroxyethyl methacrylate (HEMA), and triethylamine (TEA) were purchased from Sigma Aldrich. Sodium hydroxide, anhydrous magnesium sulfate, acetic acid, ethanol, acetone, isopropyl alcohol, and dimethylformamide (DMF) were purchased from Fisher Scientific. Hydrogen Peroxide (30%) was purchased from VWR. All purchased materials were used without further purification.

2.2. Composite Processing

2.2.1. Delignifying Pretreatment. Balsa wood sheets were cut into 100 mm × 100 mm (longitudinal × transverse) samples that were devoid of visual imperfections. Two delignifying pretreatments were used to make WTs based on previous studies, namely a chlorite-based lignin oxidation (LO) and a peroxide-based lignin modification (LM) [7,11]. For LO reactions, wood was immersed in an 80 °C

aqueous solution of 1 wt% sodium chlorite in a 1 N acetate buffer solution (sodium acetate and acetic acid, pH ~ 4.6). Oxidation proceeded until the LO-WT had become visually white (8-12 hours). For LM reactions, wood was immersed at 70 °C in an aqueous solution containing 3 wt% sodium silicate solution, 3 wt% sodium hydroxide, 0.1 wt% anhydrous magnesium sulfate, 1 wt% EDTA (used in place of referenced pentetic acid), and 4 wt% hydrogen peroxide [7]. The reaction proceeded until the LM-WT had become visually white (~2 hours). All LO- and LM-WTs were washed with hot deionized water three times to remove byproducts, followed by dehydration *via* sequential solvent exchanges from ethanol to ethanol/acetone (1:1 by volume) to acetone. Each solvent exchange was done twice for 30 min and WTs were stored in acetone at ambient conditions. Lignin content was determined by the NREL laboratory analytical procedure [32].

2.2.2. Wood Template Modification. Acetylation and methacrylation of both the LO- and LM-WTs were carried out in near identical processes with the exception of the use of acetyl vs. methacryloyl chloride reagent (AcCl vs. MeCl) and reaction temperature, 60 °C and 20 °C, respectively. Oven dried WTs were placed in a large vessel under an N_2 atmosphere prior to addition of DMF. Equivalents of AcCl/MeCl and TEA (1:1.1) added were approximated based on expected total hydroxyl content of the WT by mass, assuming glucose subunits, understanding many hydroxyl groups would be inaccessible. The acyl chlorides were added dropwise under vigorous mixing while the reaction vessel was in ice water. The vessel was removed from the ice water and the reaction proceeded for 6 hours. Modified WTs were washed in DMF, then DMF/acetone (1:1 by volume), then acetone, each washing step occurred twice. Modified WTs were dried to determine mass gains from modification then stored in acetone prior to resin infiltration. For HEMA-treated samples, unmodified WTs were dried and immersed in a HEMA bath. Vacuum was applied to ensure HEMA inclusion in the WT and visual inspection confirmed saturation prior to resin infiltration.

2.2.3 TWC Fabrication. The acetone-saturated (or HEMA-treated, in one case) delignified WTs

were submerged in the resin and degassed at 50 °C for at least 12 hours to remove acetone (or excess HEMA). The WTs were inspected for homogenous infiltration then secured between two glass panes with four 32 mm binder clips. The assembly was degassed at 50 °C for 2 hours at which point an internal white LED was illuminated for 12 hours to cure the resin. The glass panes were removed, and additional curing was done under a 405 nm lamp for 10 min at ambient conditions. For tests on pure resin, sheets were cast, degassed, and cured under identical conditions. Rectangular samples with dimensions of 63 mm × 13 mm (longitudinal × transverse) of each TWC along with the resin were cut with an Epilog Legend 36EXT laser cutter. Samples were cleaned with isopropyl alcohol to remove residues prior to any testing.

2.3. Isothermal Immersion Conditions

Isothermal water immersion conditioning was completed according to a modified ASTM D570 [33]. The isothermal water baths equilibrated at 4 °C, 20 °C, and 40 °C in airtight plastic containers for 48 hours prior to sample immersion. For each sample set, six replicates were used. The immersion samples were dried overnight in a vacuum oven at 50 °C under a 635 mm-Hg dynamic vacuum to remove all moisture and volatiles. Upon immersion, specimen masses were taken at time intervals of 30 min, 1 hr, 2 hr, 4 hr, 8 hr, 12 hr, 24 hr, 48 hr, 72 hr, 120 hr, 168 hr, 240 hr, 1 week, and once a week thereafter for 2000 hours (~83 days). For mass measurements, each specimen was removed from the water bath and dabbed with an absorbent cloth to remove superficial moisture. After samples reached their equilibrium moisture contents, all samples were dried at 50 °C for 24 hr, then another 24 hr at 50 °C overnight under a 635 mm-Hg vacuum. Measurements of water uptake with time were used to calculate water transport parameters such as kinetic rate constants, diffusion coefficients, inputs to model Fickian diffusion, and activation energies for diffusion processes (described in supporting information). Sample dimensions were taken prior to immersion, at saturation, and after drying. Length, width, and thickness were measured in triplicate at each step.

2.4. Material Characterization

2.4.1. Fourier Transform Infrared Spectroscopy (FTIR). Samples were assessed using a Cary 630 spectrometer with an Attenuated Total Reflection (ATR) accessory. FTIR was used to observe peaks associated with lignin removal or modification and identify emergence of new peaks in the WT from acetylation and methacrylation. Spectra were collected from six locations, three locations at the sample surface and three internal surfaces created via sample bisection with a razor blade. Eight scans were taken at each location from 4000 to 500 cm^{-1} at resolution of 1 cm^{-1} and averaged.

2.4.2. Thermogravimetric analysis (TGA). Auto-stepwise thermal profiles were performed with a TA Q50 using to resolve decomposition in a heterogenous composites. Under an N_2 flow rate of 40 mL/min, samples were equilibrated for 1 min at 30 °C followed by a 10 °C/min ramp rate up to 700 °C at which point a 5 min isotherm was held. During the ramp process, isotherms were triggered when the mass loss rates were > 1 wt%/min and ended when mass loss rate was < 0.1 wt%/min, at which point the temperature ramp would continue towards 700 °C.

2.4.3. Ultraviolet-visible spectroscopy (UV-Vis). Optical properties were measured using a Cary 5000 UV-Vis-NIR Spectrophotometer with a Diffuse Reflectance Accessory over a wavelength range of 300 – 800 nm at 5 nm/s using ASTM D1003 [34]. The range reported herein is 450–800 nm due to excess absorption in the materials below 450 nm. Transmittance and haze for each set of TWCs were measured prior to immersion, at saturation, and after drying. Reported values for T% and H% in materials are commonly maxima/minima or values at 550 nm due to the human eye sensitivity [35]. Maxima/minima are reported here, with 550 nm values in the supporting information.

2.4.4. Three-Point Flexural Testing. Bending tests were carried out in accordance with ASTM D7264 [36] on a 500 N load cell MTS Exceed E42. The span between supports was 52 mm, thickness to span ratio was approximately 32:1, and displacement at 1 mm/min. Specimen dimensions were taken in triplicate prior to testing. Each sample set was tested in replicates of six,

unless noted. The flexural modulus, E, and flexural strength, σ, were calculated using:

$$E = \frac{L^3 m}{4wh^3} \quad \text{Eq. 1}$$

$$\sigma = \frac{3FL}{2wh^2} \quad \text{Eq. 2}$$

where L, w, h, and F, are the span, width, thickness, and maximum force, respectively. The linear load-displacement curve slope, m, is taken between 10 – 40% the maximum force.

2.4.5. Scanning electron microscopy (SEM). Examination of the fracture surface was enabled using a Hitachi SU3500 with an operating beam voltage ranged from 10 – 25 kV. Each sample was gold coated before imaging to prevent surface charging.

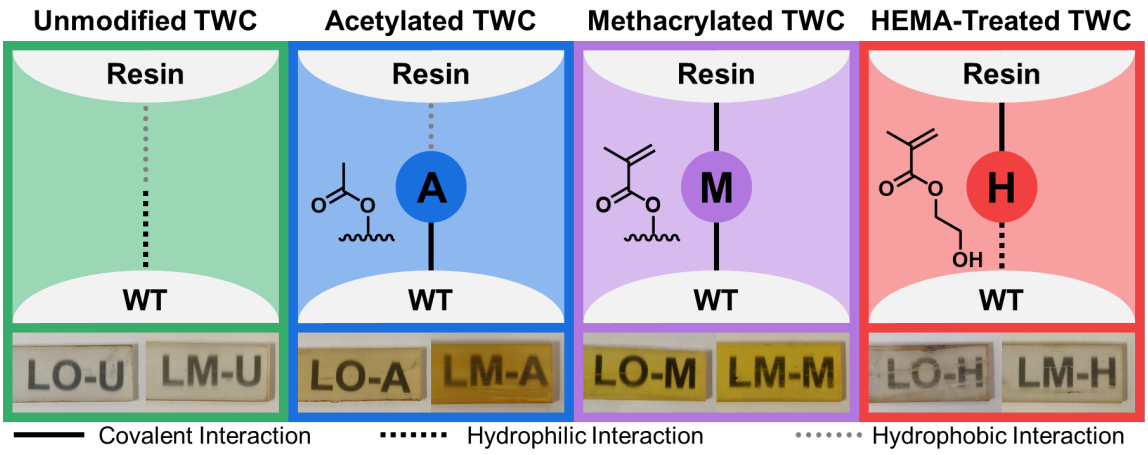

Figure 1. Proposed covalent, hydrophilic, and hydrophobic interactions between unmodified and modified WTs and resin with images of TWCs from WTs produced using the two delignifying pretreatments (LO and LM).

3. Results

3.1. Composite Processing

Example images for each type of TWC produced for this study are presented in **Figure 1**. Lignin content analysis revealed that the LO-WTs had a lignin content of 11.4% and LM-WTs had a lignin content of 20.3%, compared with 24.8% in natural balsa wood. The full biomass results are shown in **Table S1**. This result indicates that much of the lignin in LM-WTs was preserved but bleached to

remove color. Subsequent acetylation of the WTs resulted in 5–6% mass gain for both LO- and LM-WTs, similar to reported literature [6,8]. Methacrylation resulted in 12.3% mass gain in LO-WTs and 17.4% in LM-WTs, which was proportionally higher than the acetylated WTs. During the acetylation and methacrylation reactions, a brown-orange color manifested in both the LO- and LM-WTs, which has previously been reported [6,8]. Solvent washing was unsuccessful in removing the color and oxidations were not pursued due to reactivity of the methacrylate vinyl group. Mass gain from HEMA-treatment was not determined as displacement of HEMA occurs upon resin infiltration.

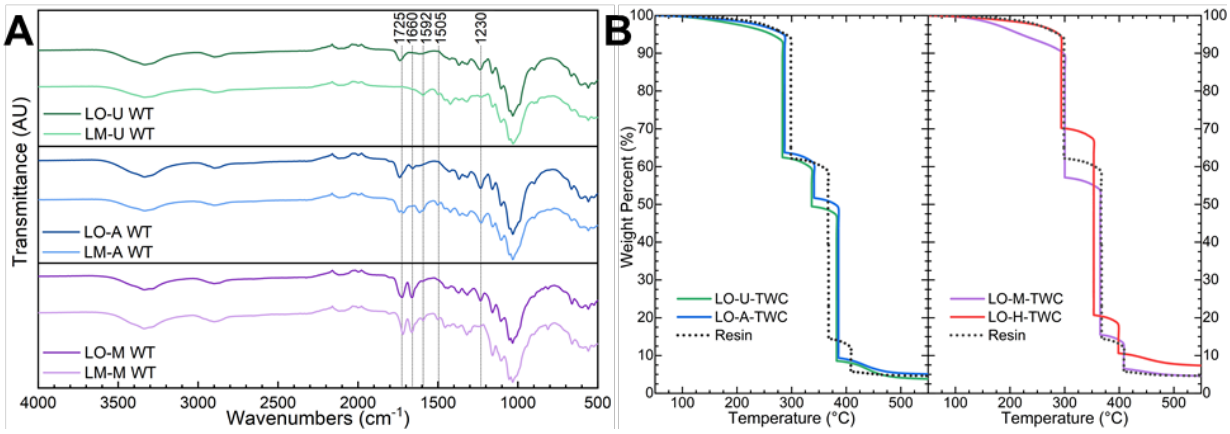

Figure 2. (a) FTIR traces for LO- and LM-WTs before modificaiton (top), acetylated (middle), and methacrylated (bottom). (b) Auto-stepwise TGA decomposition profiles for LO-TWCs with the unmodified and acetylated (left) and methacrylated and HEMA-treated (right) grouped by similarity.

3.2. Material Characterization

FTIR was used to verify delignifying pretreatments and chemical modification of the WTs with plots shown in **Figure 2a**. The LM delignifying pretreatments retained some characteristic lignin peaks around 1592 and 1505 cm^{-1}, corresponding to symmetric and asymmetric aryl ring stretching [7,37]. Acetylation and methacrylation of the WTs was successful based on the presence of a large carbonyl peak around 1730 cm^{-1} and a smaller ester linkage peak around 1230 cm^{-1}. An alkene peak is also present around 1660 cm^{-1} in methacrylated WTs. Representative TGA traces for the LO samples are shown in **Figure 2b**, the LM-TWCs had more small steps in decomposition (see

Figures S1 & S2) likely from the remaining lignin. All decomposition events occur between 275 – 500 °C, as expected for wood- and methacrylate-based materials [38,39]. The resin has two major decomposition events around 300 °C, 366 °C and a small event at 408 °C. **Figure 2b** is split to emphasize the presence of a suspected WT decomposition that occurs in LO-U and LO-A around 340 °C, but not in LO-M or LO-H, which have profiles similar to resin, with some minor shifts in temperature and weight.

UV-Vis results of maximum transmittance (T%) and minimum haze (H%) over the moisture sorption cycle are presented in a heatmap in **Figure 3**, showing desirable high T% in green and low H% in blue. Maxima and minima are reported due to variability in TWC optical response across the visible light spectrum as a result of brown-orange coloration of the WT from modification (A-TWCs and M-TWCs) and marker pigment leaching into H-TWCs during sorption testing. Values of T% and H% taken at 550 nm are available in the supporting information along with all measurements taken for each TWC (**Figures S3 – S13**) for facile comparison with literature reported values.

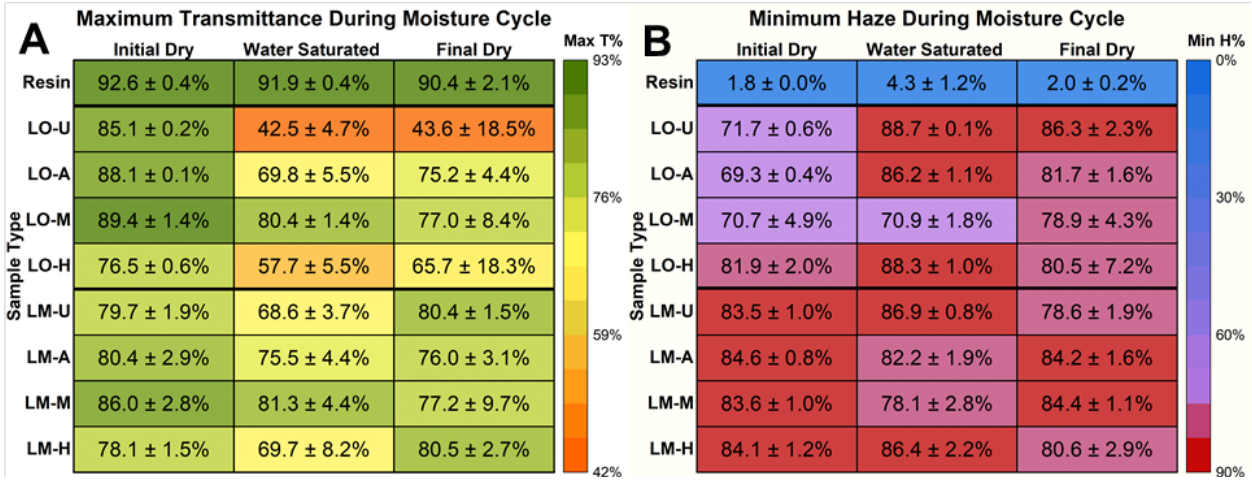

Figure 3. UV-Vis for (a) maximum transmittance values and (b) minimum haze values for the resin, LO-TWCs, and LM-TWCs at the initial dry, saturated, and final dried states, averaged across immersion temperatures (4 °C, 20 °C, and 40 °C). High transmittances (green) and low hazes (blue) are desirable.

Prior to moisture conditioning, LO-TWCs generally exhibited higher maximum T% values compared to LM-TWCs, nearly 90% for LO-M. Upon full saturation, however, LO-TWCs had a greater reduction in T% than their LM-TWC counterparts. When subsequently dried, LM-U and LM-H substantially rebounded to have higher final T% than saturated T%, where T% for LO-U remained low. The remaining lignin in LM-TWCs is thought to be responsible for the initially lower T%, due to a refractive index mismatch, and the rebounding effect. The WT modifications, specifically LO-M and LM-M, were resistant to significant reductions in T% during the sorption process and maintaining high T% upon drying. For haze, in the initial state, the LO-TWCs generally exhibited lower minimum H% than the LM-TWCs by 10.6% on average. When fully saturated with water, H% values generally went up as a result of inclusion of an additional scattering medium. Notably LO-M exhibited no change in H% and LM-A and LM-M showed slight reductions in H%, suggesting resistance to formation of scattering-sized water phases within the modified TWCs. These same modified TWCs exhibited increases in H% upon drying, while H% was reduced or unchanged in all other TWCs. Some TWCs, namely LM-U and LM-H, had H% values lower than even the initial state upon drying, showing similar rebounding effects observed in T%.

3.3. Mechanical Properties

Flexural testing was used to evaluate the influence of WT modification and moisture saturation/drying on the flexural properties of the TWCs. The flexural moduli and strengths are displayed in **Figure 4**, with force-displacement curves in the supporting information (**Figures S14 – S22**). The flexural moduli and flexural strengths of the TWCs ranged from 2.9 – 6.9 GPa and 45.8 – 92.3 MPa, respectively. These values are comparable to other flexural property values reported in the literature. For example, Li *et al.* achieved a flexural strength of 78.6 MPa and flexural modulus of 4.0 GPa for acetylated TWCs [6] and flexural strengths of 100.7 MPa for TWCs using the LM delignifying pretreatment method [7]. While the polymer phases differed from this work, they are all

PMMA-based.

In the cases of LO-U, LM-U, LO-H, and LM-H, water saturation then drying had little to no effect on flexural modulus. For LO-A, LO-M, and LM-M, small to moderate increases in modulus after water conditioning were unexpectedly observed. We hypothesize that WT swelling increased interfacial contact between chemically modified (i.e., more hydrophobic) WTs and resin, as the resin, alone, had slightly decreased moduli after water conditioning. Notably, LM-A was the only TWC to exhibit a large decrease in modulus conditioning. Generally, H-TWCs had higher moduli, followed by U-TWCs and A-TWCs with similar stiffnesses, then M-TWCs with the lowest stiffness. No significant difference in stiffness was observed based on delignifying pretreatment for LO- and LM-TWCs.

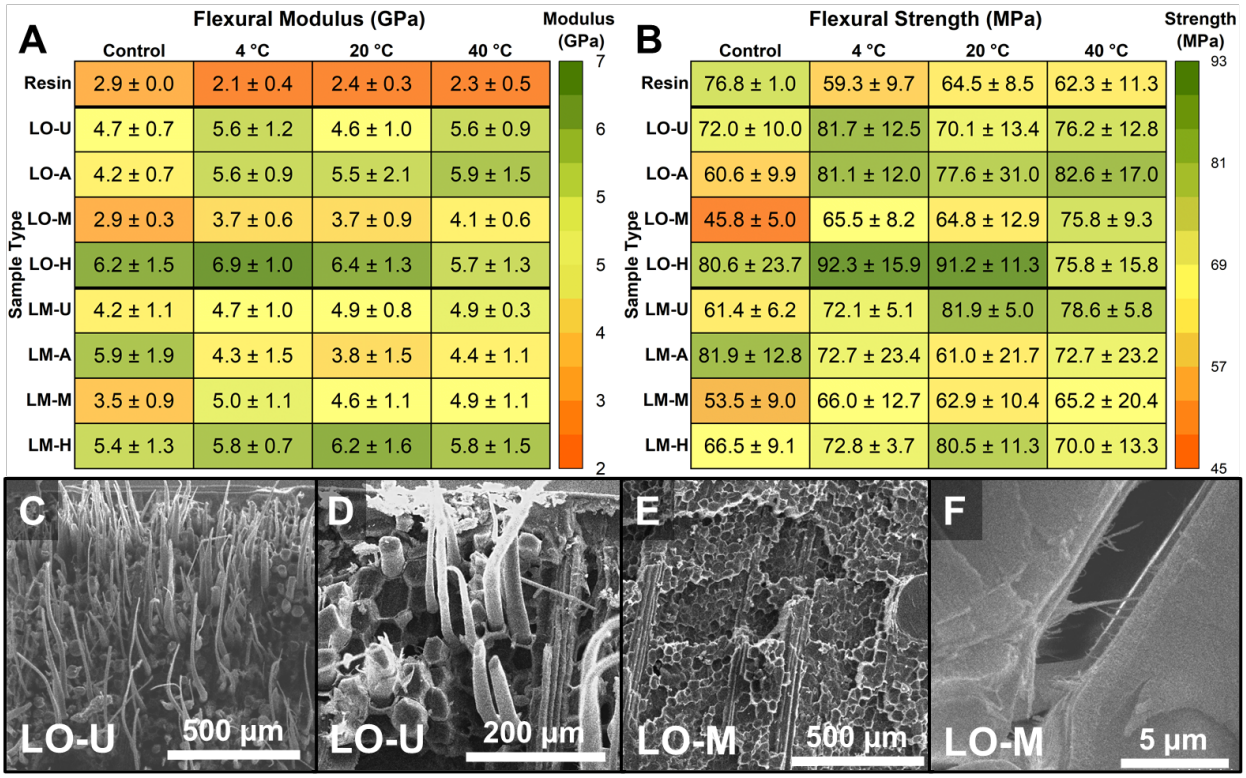

Figure 4. (a) Flexural moduli and (b) strengths for LO- and LM-TWCs, with high values in green and low values in orange. (c-f) SEM micrographs of (a, b) LO-U and (c, d) LO-M fracture surfaces.

Flexural strength was not substantially affected by water saturation followed by drying in the

cases of LO-U, LO-H, LM-M and LM-H. Like the flexural modulus, there was a slight beneficial effect from water saturation for LO-A, LO-M, and LM-U. The resin and LM-A were the only cases in which strength decreased to an observable degree with water saturation. Water conditioned LO-H was notable for exhibiting high strength compared to other TWCs, leading to the hypothesis that water acted as a plasticizer to help the HEMA establish good hydrogen bonding with the WT, specifically in the LO-WT with a lower quantity of lignin. WT modification had an effect on strength with H-TWCs, A-TWCs, and U-TWCs exhibiting similar strengths while M-TWCs were weaker.

3.4. Scanning Electron Microscopy of Fracture Surfaces

SEM analysis was used to observe the fracture surfaces of TWCs after flexural testing. For brevity, we highlight only two TWC types, LO-U and LO-M, that exhibit the largest consistent contrast in failure modes, simple tension and brash tension, respectively. All other TWC types exhibited a combination of failure modes and fracture surfaces that had features in between that of LO-U and LO-M. Failure surface images are shown in **Figure 4c-f**. LO-U failure surfaces comprised long, tapered fibers of resin emerging from cell lumina (**Figure 4c,d**) instead of splintered wood fibers, typical of wood failure in bending. In contrast, LO-M fracture surfaces were smooth, corresponding to brash fracture. Examining the WT–resin interface for the LO-M specimen showed fibers spanning across a gap created during failure (**Figure 4f**), suggesting failure of the cell wall rather than delamination between the WT and resin. Cell wall failure in LO-M samples would indicate strong adhesion, perhaps covalent bonding, between the resin and modified WT.

3.5. Isothermal Water Sorption

During isothermal moisture conditioning, mass uptake was measured at regular time intervals until equilibrium was reached. Representative sorption curves for some LO-TWC samples are

shown in **Figure 5a** (all curves found in **Figures S23 – S25**). Four out of 144 TWC samples split longitudinally during moisture conditioning. Three were LO-H at 4 °C (approx. 2, 500, and 800 hr) and one was LO-H at 40 °C (approx. 2 hr). The two samples that failed at 2 hr were not used for any calculations. The two samples that failed around 500 and 800 hr were used for water transport parameter calculations, as sorption behavior prior to failure was not abnormal. None of the four failed samples were used for mechanical testing. LO-H TWCs were particularly susceptible to swelling with some achieving 20% volume increases at saturation (**Figure S26b**). The large swelling in the H-TWCs is a result of the native water sorption properties of HEMA, absorbing up to 0.6 $g_{water}/g_{poly(HEMA)}$ in water immersion conditions [40]. Dimension changes with water sorption and desorption, along with anti-swelling and anti-shrinkage efficiencies, are provided in the supporting information, (**Figures S26 – S30**).

At longer sorption times for the M-TWCs, net mass uptake decreased without apparent changes in sample integrity, the highest being LO-M at 40 °C losing 4% of its gained mass. Similar behavior has been reported during sorption due to matrix sloughing [25,41]. Overt matrix sloughing was not visibly apparent in this work, yet some chemical or physical break-down was occurring [42]. Post-dried net mass changes revealed losses of 2 – 7% among all TWCs and < 1% gains in resin (**Figure S31**). The small mass loss in the TWCs could arise from fragmented components of the wood templates as the resin saw a small net mass gain. The lost mass represented around 100 mg of the sample weight in the most extreme case. The moisture resistance of the M-TWCs was more sensitive to detecting these mass losses, indicated by a decrease in the moisture sorption curve in **Figure 5a**.

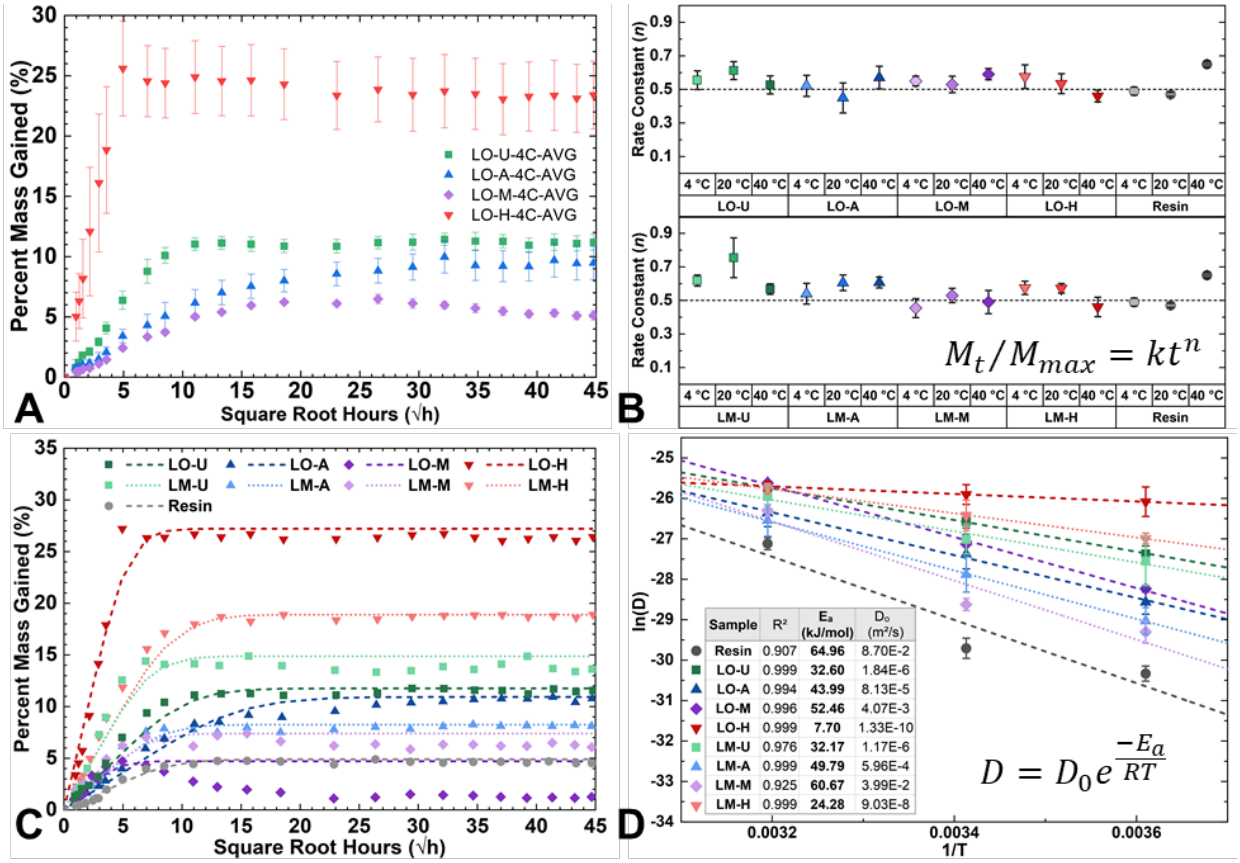

Figure 5. (a) Example sorption curves by modification type of LO at 4 °C. (b) Kinetic exponential term (*n*) for LO-TWCs (top) and LM-TWCs (bottom), with *n*~0.5 indicating Fickian behavior. (c) Experimental sorption plots for individual specimens (scatter) overlaid with diffusion model outputs (dashed line). (d) Temperature-dependent Arrhenius relations for LO-TWCs and LM-TWCs with calculated values for activation energy (E_a) and permeability index (D_0).

Maximum moisture contents, M_{max}, in TWCs can be broadly grouped by modification, with M-TWCs between 5 – 8%, A-TWCs from 9 – 14%, U-TWCs between 11 – 15%, and H-TWCs ranging 15 – 27%. The resin absorbed around 5%, indicating good sorption resistance by M-TWCs. Among H-TWCS, LO-H absorbed >20% in each case, unsurprising with HEMA, but LM-H samples absorbed between 15 – 18%, suggesting some additional moisture resistance imparted by remaining lignin. It is known that the M_{max} for WPCs will depend on fiber morphology, quantity, and matrix material. Ranges of M_{max} observed in this study (5 – 27%) are within ranges found in other WPC

literature (2 – 40%) [25,26].

3.6. Kinetic Rate Constants of Diffusion

Calculated kinetic rate constants for all TWCs and the resin are shown in **Figure 5b** and plots related to determination of n and k for each sample are shown in **Figures S32 – S40**. As detailed in the supporting information, the time exponential term, n, is a convenient means to categorize diffusion. Values of $n \approx 0.5$ indicate Fickian diffusion, $n \approx 1$ represent relaxation-controlled diffusion, and values of $0.5 < n < 1$ represent anomalous diffusion. All TWCs exhibit near-Fickian diffusion behavior, with a minimum value of $n = 0.45$ (LO-A at 20 °C) and a maximum value of $n = 0.75$ (LM-U at 20 °C), which was an outlier, given the next highest value of $n = 0.65$ (Resin at 40 °C). Most values were 0.5 – 0.6, indicating that, although there is some anomalous behavior, diffusion in TWCs exhibit more Fickian than relaxation-controlled water diffusion behavior.

3.7. Moisture Diffusion Coefficients

Diffusion coefficients for each sample are reported in **Table 1** along with the parameters required for their calculation. For clarity and brevity, in text usage of "D" will have implied units of ($\times 10^{-13}$ m^2/s), consistent with **Table 1**. The initial, linear slopes of experimental sorption curves, θ, can be found in **Figures S41 – S49**. Compared with resin, the TWCs exhibited higher diffusivities in every instance, which was expected in a composite with lignocellulosic filler. For example, at 4 °C, $D = 0.67$, $D = 12.97$, $D = 10.86$, for Resin, LO-U, and LM-U, respectively. As expected, data show a temperature-dependence of the diffusion coefficients for each sample formulation. For example, LO-M exhibited increases in diffusivity with temperature from $D = 5.47$ at 4 °C, to $D = 16.52$ at 20 °C, to $D = 74.78$ at 40 °C. This increase in thermal energy enables rapid transport of water into the wood-polymer composite and is consistently observed in the literature [22,23,25,26,42].

The delignifying pretreatments (LO vs. LM) affected diffusivity, where LO-TWCs had higher diffusivities than LM-TWCs at every level of modification and temperature, likely from the high

lignin content in LM-TWCs resisting moisture intrusion. Lowering the lignin content in wood and other lignocellulosic materials has been shown to increase diffusivity [43,44]. Diffusivity was also affected by WT modification, where H-TWCs, treated with hydrophilic HEMA, exhibited substantial increases in diffusivity relative to the U-TWCs, with D = 46.90 and D = 18.91 at 4 °C for LO-H and LM-H, respectively. In the cases of A-TWCs and M-TWCs, the diffusivities were lower than the U-TWCs indicating that these chemical modifications successfully mitigated moisture intrusion. For example, at 20 °C, D = 18.65, D = 7.77, and D = 3.70 for LM-U, LM-A, and LM-M, respectively. For the M-TWCs, specifically, there were substantial differences in diffusivity between LO-M and LM-M, where at each temperature case, LO-M was at least two times greater than LM-M. Although a broad range of diffusion coefficients are report here, similar spans of magnitude in diffusivities have been reported in the WPC literature, with ranges between D = 0.32 [26] and D = 420 [42] that depend on a multitude of factors.

Table 1. Maximum Moisture and Diffusion Coefficients

Sample	T (K)	M_{max} (%)	h_0 (mm)	θ ($\times 10^{-2}$ $h^{-0.5}$)	D_A ($\times 10^{-13}$ m^2/s)	ECF	D ($\times 10^{-13}$ m^2/s)
	277	5.0 ± 0.5	1.66	0.12 ± 0.01	0.90 ± 0.17	1.34	0.67 ± 0.13
Resin	293	6.0 ± 0.7	1.62	0.20 ± 0.01	1.68 ± 0.38	1.33	1.26 ± 0.27
	313	4.6 ± 0.3	1.67	0.56 ± 0.04	22.44 ± 3.80	1.34	16.69 ± 2.48
	277	11.5 ± 0.6	1.64	1.20 ± 0.11	17.32 ± 3.40	1.33	12.97 ± 2.48
LO-U	293	12.2 ± 1.4	1.64	2.00 ± 0.39	38.70 ± 6.07	1.34	28.99 ± 2.64
	313	12.2 ± 2.2	1.69	2.90 ± 0.61	89.10 ± 13.50	1.35	66.13 ± 9.81
	277	9.8 ± 1.4	1.66	0.57 ± 0.11	5.27 ± 1.61	1.34	3.93 ± 1.19
LO-A	293	13.6 ± 2.1	1.67	1.40 ± 0.42	17.25 ± 5.38	1.34	12.84 ± 3.99
	313	9.3 ± 2.0	1.64	1.60 ± 0.18	47.27 ± 18.46	1.34	35.54 ± 14.44
	277	6.5 ± 0.4	1.76	0.43 ± 0.01	7.44 ± 0.60	1.36	5.47 ± 0.45
LO-M	293	5.9 ± 0.3	1.75	0.68 ± 0.04	22.54 ± 5.36	1.36	16.52 ± 3.74
	313	4.7 ± 0.1	1.77	1.20 ± 0.04	102.11 ± 5.76	1.37	74.78 ± 3.67
	277	25.9 ± 3.3	1.48	5.90 ± 2.10	60.85 ± 25.82	1.30	46.90 ± 20.52
LO-H	293	26.7 ± 1.1	1.50	6.50 ± 1.00	73.35 ± 15.39	1.31	56.18 ± 11.95
	313	20.3 ± 4.4	1.51	5.40 ± 0.95	90.05 ± 11.05	1.31	68.90 ± 8.26
	277	14.8 ± 5.6	1.70	1.50 ± 1.00	14.55 ± 9.23	1.35	10.86 ± 6.98
LM-U	293	13.3 ± 4.8	1.67	1.70 ± 0.74	24.94 ± 8.27	1.34	18.65 ± 6.31
	313	11.6 ± 3.9	1.72	2.50 ± 1.10	72.52 ± 18.93	1.35	53.74 ± 14.41
	277	14.1 ± 1.6	1.70	0.65 ± 0.09	3.39 ± 1.39	1.35	2.47 ± 0.86
LM-A	293	12.4 ± 3.2	1.77	0.95 ± 0.28	10.67 ± 5.30	1.36	7.77 ± 3.70
	313	8.8 ± 1.8	1.82	1.30 ± 0.29	41.16 ± 13.97	1.37	29.61 ± 9.45

	277	8.2 ± 0.7	1.63	0.34 ± 0.06	2.50 ± 0.61	1.33	1.88 ± 0.46
LM-M	293	7.4 ± 0.7	1.61	0.43 ± 0.03	4.91 ± 0.78	1.33	3.70 ± 0.59
	313	6.0 ± 0.8	1.65	1.10 ± 0.07	50.74 ± 6.84	1.34	37.94 ± 5.13
	277	17.7 ± 1.9	1.56	2.40 ± 0.24	24.89 ± 3.14	1.32	18.91 ± 2.55
LM-H	293	17.1 ± 1.0	1.57	3.10 ± 0.55	44.43 ± 12.76	1.32	33.65 ± 9.74
	313	15.0 ± 1.0	1.54	3.90 ± 0.32	85.90 ± 11.05	1.31	65.29 ± 7.80

3.8. Fickian Diffusion Model

As a result of dominantly Fickian behavior exhibited by the TWCs, we applied a one-dimensional Fickian diffusion model, described in the supporting information. The model was evaluated over time intervals identical to experimental data. Each of the predicted diffusion curves were overlaid onto the experimental sorption data, with representative examples shown in **Figure 5c**, with the complete series available in **Figures S50–S58.** Readily observed is some variability in "goodness-of-fit" between samples, with most experimental scatter data sitting on or near the predicted line except for LO-M where mass uptake decreases at longer times. Since the model outputs were time-matched to experimental data, RMSE was calculated for all TWCs to quantitatively evaluate "goodness-of-fit." RMSE has the same units as the comparison values, in this case it is fractional mass gain (0 to 1 scale), where larger values indicate larger deviations. Most samples were below an RMSE value of 0.15 with a few outliers among sample types, indicating relatively good model fits (full data available in **Figure S59**). The largest deviations between experimental data and the model occur in the plateau region of sorption curves, rather than in the early sorption phase. Generally, LO-TWCs exhibited a lower and narrower range of RMSE values, except for LO-M. The decreasing mass observed in LO-M TWCs, coupled with already low moisture uptakes, led to large, temperature-dependent RMSE values, reaching between 0.5–0.65 for LO-M at 40 °C. The LM-TWCs showed some temperature dependent deviations in the cases of LM-U, LM-M, and LM-H. The RMSE for resin was low across all temperatures with good agreement with the model, indicating that the wood-based templates and the interaction with the resin were likely the primary sources of deviation from the model.

3.9. Thermodynamics of Diffusion

Activation energies of diffusion were calculated using an Arrhenius rate law (detailed in supporting information) applied to the diffusion coefficients at varying temperature. The Arrhenius relationships are shown graphically, and relevant parameters tabulated in **Figure 5d**. E_a provides a quantitative measure of the inherent water resistance of a material, which enables direct comparison between modified material systems. The activation energies of unmodified and modified TWCs ranged from 7.7 – 60.7 kJ/mol, and the E_a of the resin was 64.96 kJ/mol, which was higher than any of the TWCs, as expected. Srubar *et al.* similarly showed that silane modification of lignocellulosic filler or maleate modification of the matrix polymer were effective methods to inhibit water transport in wood-flour/poly(hydroxyalkanoate) composites, with E_a ranges spanning 18 – 50 kJ/mol for unmodified and modified composites and 56 kJ/mol for the matrix polymer [26].

Increased activation energy of diffusive processes is directly related to a decrease in the kinetic rate of water transport (i.e., increased moisture resistance), which was a primary goal in this study. In nearly every case, LM-TWCs exhibited higher activation energies of diffusion than LO-TWCs. The exception to this trend concerns LM-U and LO-U, which were comparable at 32.17 and 32.60 kJ/mol, respectively. Trends in E_a for the template modifications were consistent across LM and LO, where M-TWCs had the highest E_a, followed by A-TWCs, then U-TWCs. H-TWCs had the lowest values of E_a, which correlates with the high M_{max} and high diffusion coefficients for the hydrophilic additive. Taken together, these results demonstrate a multifaceted approach to increase activation energy of diffusion, and therefore moisture resistance through initial WT treatment, as in the case of delignifying pretreatment, and through subsequent chemical modification.

4. Discussion

Delignifying pretreatment and interfacial modifications of the WT prior to resin infiltration substantially affected the optical, mechanical, and water diffusion behavior of TWCs. The TWCs

largely followed Fickian diffusion behavior when subjected to water immersion conditions. A characteristic Fickian diffusion model was applied to the TWCs with good agreement with experimental sorption behavior in most cases. There were some cases where anomalous behavior was observed ($n > 0.6$), but deviations were not consistent across temperatures or type of TWC.

Covalent grafting of hydrophobic and crosslinking groups on the WT (acetylation and methacrylation) successfully reduced water transport when compared to the unmodified, U-TWCs by decreasing the M_{max}, reducing diffusion coefficients, and increasing the E_a required for diffusion processes. Specifically, the M-TWCs increased E_a of diffusion close to that of the resin, which had an E_a twice that of the U-TWCs. The M-TWCs and A-TWCS exhibited lower moduli of elasticity and lower strength than the U-TWCs or H-TWCS, which was likely due to the hydrophobic covalent grafts disrupting interchain hydrogen bonding within the wood template [8,29]. Despite the coloration imparted to the WT from the chemical modifications, M-TWCs had high maximum T% and low minimum H% when saturated with water, further indicating moisture resistance. Compatibilization of the resin and the WT in LO-M was evidenced by similarity in thermal decomposition where LO-U and LO-A exhibited an additional decomposition step, thought to be the WT. Additionally, uniform brash failure of M-TWCs in bending, with fibers bridging a gap under SEM suggest strong WT-resin interactions. LO-M exhibited poor fitting with the Fickian Model because mass was leached during moisture conditioning, indicated by a decrease on the moisture absorption curve rather than a plateau. Despite each TWC losing some amount of its original mass from leaching during moisture conditioning (see Figure S31), LO-M was sensitive to this leaching due to its low water uptake.

HEMA-treating the WT aimed to promote hydrogen bonding with the WT and polymerization with the resin to circumvent some detriments of covalent grafting to the WT (e.g. diminished mechanics, WT coloration, additional processing steps). HEMA-treatment served to substantially

increase water transport processes in the resulting TWCs, which was expected for a hydrophilic additive. H-TWCs exhibited large M_{max}, high diffusion coefficients, low E_a, and substantial dimensional changes when subjected to water immersion conditions. Notably, the only four TWCs to fail during water sorption were LO-H, likely due to excessive swelling. The H-TWCs, generally, had higher elastic moduli than other TWCs and demonstrated some optical rebounding where T% was reduced with water saturation and regained when dried. These results suggest favorable and perhaps, dynamic interfacial interactions, despite poor sorption performance.

The selected delignifying pretreatments (LO vs. LM) had less of an effect on the optical, mechanical, and moisture diffusion properties compared to interfacial modifications, but some effects were notable. Generally, LO-TWCs had higher initial T% and lower initial H% when compared to LM-TWCs, but upon moisture saturation and drying, the benefits were negated. LM-U exhibited similar optical rebounding effects to the H-TWCs, while LO-U saw substantial, permanent decreases in T% with moisture saturation. There were no substantial differences in flexural properties between LM- and LO-TWCs. LM-TWCs were more resistant to water transport, exhibiting lower diffusion coefficients and higher E_a for diffusion processes when compared to LO-TWCs, indicating a water transport resistance likely due to the high lignin content remaining in the LM-TWCs.

5. Conclusions

This study serves as an initial investigation into characterizing water transport properties in TWCs and strategies to mitigate moisture-induced deterioration while improving other material properties of interest. Much of the work regarding TWCs emphasizes applications in windows and photovoltaics, where durability in aggressive, moisture-rich environments is required. Understanding the effects of WT modification on basic properties of TWCs serves to better tailor these composites for longevity in the proposed applications.

In this work, TWCs were produced using two delignifying pretreatments of balsa wood and three interfacial modifications that affected hydrophobic (acetylation, A-TWCs), hydrophilic (HEMA-treatment, H-TWCs), and covalent (methacrylation, M-TWCs) interactions between the wood template and the infiltrating methacrylate polymer. These modified TWCs were subjected to isothermal water immersion conditions and largely followed Fickian diffusion behavior. A characteristic Fickian diffusion model was applied to the TWCs with good agreement with experimental sorption behavior in most cases. The delignifying pretreatments had modest influences on the water sorption behavior, where LM-TWCs, containing higher lignin contents, exhibited increased resistance to water transport. Covalent grafting of hydrophobic (A-TWCs) and crosslinking (M-TWCs) groups on the WT successfully reduced water transport and increased the activation energy of diffusion when compared to the unmodified (U-TWCs). Water saturation with subsequent drying had a minimal effect on the mechanical properties of the TWCs. In all cases, water sorption/desorption affected the optical properties of the TWCs, but some TWCs were able to regain optical properties when subsequently returned to a desiccated state.

In the emerging field of TWCs, methacrylation of the WT and inclusion of HEMA are new modification strategies that demonstrated select advantages. M-TWCs showed reduced moisture uptake (<10%), the highest activation energy for diffusion (>50 kJ/mol), and a resistance to moisture-induced optical deterioration, evidenced by little change in transmittance and haze when fully saturated with water. In contrast, the H-TWCs, despite having higher moisture absorption, resisted moisture-induced mechanical deterioration, exhibiting higher stiffnesses and strengths after drying relative to the other TWCs.

Acknowledgements

This research was made possible by the Department of Civil, Environmental, and Architectural Engineering, the College of Engineering and Applied Sciences, and the Living Materials Lab at the

University of Colorado Boulder and the Miyake Research Group at Colorado State University.

References

[1] S. Fink, Transparent Wood - A New Approach in the Functional Study of Wood Structure, Holzforschung. 46 (1992) 403–408.

[2] Y. Li, Q. Fu, S. Yu, M. Yan, L. Berglund, Optically Transparent Wood from a Nanoporous Cellulosic Template: Combining Functional and Structural Performance, Biomacromolecules. 17 (2016) 1358–1364.

[3] M. Zhu, *et al.*, Highly Anisotropic, Highly Transparent Wood Composites, Adv. Mater. 28 (2016) 5181–5187.

[4] T. Li, *et al.*, Wood Composite as an Energy Efficient Building Material: Guided Sunlight Transmittance and Effective Thermal Insulation, Adv. Energy Mater. 6 (2016) 1601122.

[5] Y. Li, E. Vasileva, I. Sychugov, S. Popov, L. Berglund, Optically Transparent Wood: Recent Progress, Opportunities, and Challenges, Adv. Opt. Mater. 6 (2018) 1800059.

[6] Y. Li, X. Yang, Q. Fu, R. Rojas, M. Yan, L.A. Berglund, Towards centimeter thick transparent wood through interface manipulation, J. Mater. Chem. A. 6 (2017) 1094–1101.

[7] Y. Li, Q. Fu, R. Rojas, M. Yan, M. Lawoko, L. Berglund, Lignin-Retaining Transparent Wood, ChemSusChem. 10 (2017) 3445–3451.

[8] K. Foster, K.M. Hess, G.M. Miyake, W.V. Srubar, Optical Properties and Mechanical Modeling of Acetylated Transparent Wood Composite Laminates, Materials (Basel). 12 (2019) 2256.

[9] E. Vasileva, *et al.*, Light Scattering by Structurally Anisotropic Media: A Benchmark with Transparent Wood, Adv. Opt. Mater. 6 (2018) 1800999.

[10] H. Chen, *et al.*, Thickness Dependence of Optical Transmittance of Transparent Wood: Chemical Modification Effects, ACS Appl. Mater. Interfaces. 11 (2019) 35451–35457.

[11] A. Subba Rao, G. Nagarajappa, S. Nair, A. Chathoth, K.K. Pandey, Flexible transparent wood

prepared from poplar veneer and polyvinyl alcohol, Compos. Sci. Technol. 182 (2019) 107719.

[12]W. Gan, S. Xiao, L. Gao, R. Gao, J. Li, X. Zhan, Luminescent and Transparent Wood Composites Fabricated by Poly(methyl methacrylate) and γ-Fe 2 O 3 @YVO 4 :Eu 3+ Nanoparticle Impregnation, ACS Sustain. Chem. Eng. 5 (2017) 3855–3862.

[13]Z. Yu, *et al.*, Transparent Wood Containing CsxWO3 Nanoparticles for Heat-Shielding-Window Applications, J. Mater. Chem. A. 5 (2017) 6019–6024.

[14]Q. Fu, M. Yan, E. Jungstedt, X. Yang, Y. Li, L.A. Berglund, Transparent plywood as a load-bearing and luminescent biocomposite, Compos. Sci. Technol. 164 (2018) 296–303.

[15]M. Zhu, *et al.*, Anisotropic, Transparent Films with Aligned Cellulose Nanofibers, Adv. Mater. 29 (2017) 1606284.

[16]H. Yaddanapudi, N. Hickerson, S. Saini, A. Tiwari, Fabrication and characterization of transparent wood for next generation smart building applications, Vac. 146 (2017) 649–654.

[17]M. Zhu, *et al.*, Transparent and haze wood composites for highly efficient broadband light management in solar cells, Nano Energy. 26 (2016) 332–339.

[18]Q. Lin, X. Zhou, G. Dai, Effect of hydrothermal environment on moisture absorption and mechanical properties of wood flour-filled polypropylene composites, J. Appl. Polym. Sci. 85 (2002) 2824–2832.

[19]V. Steckel, C. Clemons, H. Thoemen, Effects of Material Parameters on the Diffusion and Sorption Properties of Wood-Flour/Polypropylene Composites, J. Appl. Polym. Sci. 103 (2007) 752–763.

[20]A. Ashori, A. Nourbakhsh, Reinforced polypropylene composites: Effects of chemical compositions and particle size, Bioresour. Technol. 101 (2010) 2515–2519.

[21]B. Tisserat, L. Reifschneider, D. Grewell, G. Srinivasan, Effect of particle size, coupling agent and DDGS additions on Paulownia wood polypropylene composites, J. Reinf. Plast. Compos.

33 (2014) 1279–1293.

[22]A. Espert, F. Vilaplana, S. Karlsson, Comparison of water absorption in natural cellulosic fibres from wood and one-year crops in polypropylene composites and its influence on their mechanical properties, Compos. Part A Appl. Sci. Manuf. 35 (2004) 1267–1276.

[23]M.S. Islam, K.L. Pickering, N.J. Foreman, Influence of Hygrothermal Ageing on the Physico-Mechanical Properties of Alkali Treated Industrial Hemp Fibre Reinforced Polylactic Acid Composites, J. Polym. Environ. 18 (2010) 696–704.

[24]K.M. Hess, W. V. Srubar, Activating relaxation-controlled diffusion mechanisms for tailored moisture resistance of gelatin-based bioadhesives for engineered wood products, Compos. Part A Appl. Sci. Manuf. 84 (2016) 435–441.

[25]S.J. Christian, S.L. Billington, Moisture diffusion and its impact on uniaxial tensile response of biobased composites, Compos. Part B Eng. 43 (2012) 2303–2312.

[26]W. V. Srubar, C.W. Frank, S.L. Billington, Modeling the kinetics of water transport and hydroexpansion in a lignocellulose-reinforced bacterial copolyester, Polymer (Guildf). 53 (2012) 2152–2161.

[27]J. George, M.S. Sreekala, S. Thomas, A Review on Interface Modification and Characterization of Natural Fiber Reinforced Plastic Composites, Polym. Eng. Sci. 41 (2001) 1471–1485.

[28]P. V. Joseph, M.S. Rabello, L.H.C. Mattoso, K. Joseph, S. Thomas, Environmental effects on the degradation behaviour of sisal fibre reinforced polypropylene composites, Compos. Sci. Technol. 62 (2002) 1357–1372.

[29]M.J. Ramsden, F.S.R. Blake, N.J. Fey, The effect of acetylation on the mechanical properties, hydrophobicity, and dimensional stability of *Pinus sylvestris*, Wood Sci. Tech. 31 (1997) 97–104.

[30]B.K. Segerholm, P. Walkenström, B. Nyström, M.E.P. Wålinder, P. Larsson Brelid, Micromorphology, moisture sorption and mechanical properties of a biocomposite based on

acetylated wood particles and cellulose ester, Wood Mater. Sci. Eng. 2 (2007) 106–117.

[31]T. Keplinger, E. Cabane, M. Chanana, P. Hass, V. Merk, N. Gierlinger, I. Burgert, A versatile strategy for grafting polymers to wood cell walls, Acta Biomater. 11 (2015) 256–263.

[32]ASTM Standard D570, Standard Test Method for Water Absorption of Plastics, 2018.

[33]ASTM Standard D1003, Standard Test Method for Haze and Luminous Transmittance of Transparent Plastics 1, 2013.

[34]R.A. Weale, The Foveal and Para-Central Spectral Sensitivities in Man, J. Physiol. 114 (1951) 435–446.

[35]ASTM Standard D7264, Standard Test Method for Flexural Properties of Polymer Matrix Composite Materials 1, 2015.

[36]U.P. Agarwal, R.H. Atalla, Chapter 4: Vibrational spectroscopy, in: Lignin Lignans Adv. Chem., 2010: pp. 104–136.

[37]L. Tranvan, V. Legrand, F. Jacquemin, Thermal decomposition kinetics of balsa wood: Kinetics and degradation mechanisms comparison between dry and moisturized materials, Polym. Degrad. Stab. 110 (2014) 208–215.

[38]P. Gałka, J. Kowalonek, H. Kaczmarek, Thermogravimetric analysis of thermal stability of PMMA films modified with photoinitiators, J. Therm. Anal. Calorim. 115 (2014) 1387–1394.

[39]C.L. Lewis, M. Anthamatten, Synthesis, swelling behavior, and viscoelastic properties of functional poly(hydroxyethyl methacrylate) with ureidopyrimidinone side-groups, Soft Matter. 9 (2013) 4058–4066.

[40]A.C. Loos, G.S. Springer, B.A. Sanders, R.W. Tung, Moisture Absorption of Polyester-E Glass Composites, J. Compos. Mater. 14 (1980) 142–154.

[41]V.A. Alvarez, A. Vázquez, Effect of water sorption on the flexural properties of a fully biodegradable composite, J. Compos. Mater. 38 (2004) 1165–1182.